

For references, quote as:

Pablo Baquero, Effimia Giannopoulou, Alberto T. Estévez, "A Unified Force Driven Design for Additive Manufacture Large Scale Structures Using Particle Spring Systems", in Alberto T. Estévez (ed.), *4<sup>th</sup> International Conference for Biodigital Architecture & Genetics*, iBAG-UIC Barcelona, Barcelona, 2020, pp. 273-286. ISBN: 978-84-09-22004-5. Dep. Leg. B 13784-2020.

Available in: <https://www.bubok.es>.

## **"A Unified Force Driven Design for Additive Manufacture Large Scale Structures Using Particle Spring Systems"**

Pablo Baquero, Effimia Giannopoulou, Alberto T. Estévez, iBAG-UIC Barcelona

### **Abstract**

This article introduces a design approach for generating complex geometries, especially for the purpose of additive manufacturing large physical objects with Fused Filament Fabrication process. The case studies are focused on the process for the design and 3D print of functional furniture as a single piece in 1:1 scale inspired by natural phenomena such as the capillary bridges. By interactively controlling the geometry, as one continuous element in equilibrium, dynamic relaxation using particle spring systems with different warps and wefts forces is used to adjust geometry and overhangs, balancing internal structure, economizing material and travelling time. The benefits of programming the curves with forces and printing paths can enhance the workflow of design directed especially for fabrication. The *Radiolaria* and *Hyperboloid Series* of furniture are presented here as an outcome of this research.

### **Keywords**

Additive manufacturing; Capillary bridges; Dynamic relaxation; Digital organicism; Biodigital architecture; Furniture design; Digital design; Digital manufacturing; Bio-learning.

### **Introduction**

"Design for manufacturing involves simultaneously considering design goals and manufacturing constraints in order to identify manufacturing problems while parts are being designed" (Gupta et al., 1997). Specifically, responding to the challenge to design for additive manufacturing (AM) rather than 3D print a design, the fabrication method and materiality establish the generative design constraints that inform the geometry (Huang, 2016). Based on Thomson's (2016) guidelines, this should involve designing and optimizing a product together with its production system to reduce development time and cost. Inside this context, this investigation is examining a generative design process for large scale additive manufacturing of thin shells or hollow structures.

In an effort to provide, as Mies van der Rohe and Le Corbusier have achieved, a typological search that could configure architecture and design with the tools and possibilities of the 21st century, this article exemplifies a specific line of furniture that is being developed in the Institute for Biodigital Architecture & Genetics at UIC, Barcelona.

The three case studies presented here are analyzed from the perspective of design aspects and analysis tools, directed specifically for manufacturing using the Fused Filament Fabrication (FFF) process, an alternative term of the Fused Deposition Modeling. The case studies demonstrate final furniture design products. However, the design methodology could be extended to architectural scales for additive manufacturing using similar emerging technologies. This article presents a coherent design methodology, tested solutions and considerations for the development of the final outcomes.

## **State of Problem**

Generally, design for manufacturing monolithic structures has more advantages and potentials compared to the complex assemblies of modular parts, which have to be mounted considering tolerance factors and the connection system amongst others. Designing a large single piece for AM though, has its own process limitations and requirements and the design method has to be conceptualized based on those constraints, and with most important the size of the printer.

In addition, the deposition of a layer-by-layer material technique causes the staircase or stair-step effect which is common in all rapid prototype processes. During the FFF process, it becomes more apparent, as in the case of large-scale objects with curved surfaces, particularly because of using thicker layers (larger nozzle). The main source of this effect in most rapid prototype systems, is the weakness of the stereolithography (.STL) files produced by software and especially the approximations of the curved surface of the layer with a uniform thickness (Nasr et al., 2014).

Furthermore, in the case of thin shell surfaces with mean curvature near zero (minimal surfaces), slicing produces gaps at the saddle shaped areas of the surfaces. Also, overhangs appear at the locations with angles smaller than 45 degrees, and integral reinforcement is required in the inner hollow space. Moreover, investigators have also emphasized shrink or warp deformations issues, due to the temperature gradients the deposition process involves (Alsoufi & Elsayed, 2017) and interlayer bonding weaknesses, especially in 3D construction printing (Marchment, 2019; [1]). In general, layer height and feed rate influence the mechanical behavior of parts (Chacón et al., 2017). In the case of large-scale shell objects with complex geometry those effects could become more obvious.

Another important factor is that commercially available topology optimization tools are able to minimize the weight of the object, but do not yet consider FFF limitations (e. g. overhangs, thin walls), which could lead to over 55% of build time going into fabrication of support structures. In this case, the designer needs to change the geometry to reduce overhangs and to consider the build orientation in the early design stage to avoid support structure. Generative design tools could help integrate those constraints inside the design process (Simpson, 2019).

“In general, any amount of time the printer spends moving without printing is considered wasted time, because the part isn’t being constructed. In addition, the start/stop point, known as the seam, is often a blemish on the surface of the part that contributes to weaker material properties” (Roschli et al., 2019). Some successful solutions propose a method of modifying the CAD file and slicing engine to allow for parts to be printed without starting and stopping the extruder, by controlling the seam, and the realization of single-continuous paths that avoid material collisions and crossovers (Gupta & Krishnamoorthy, 2019).

#### *Adaptive tool path strategies*

Nowadays, researchers are proposing different solutions of slicing algorithms to improve the boundary contour’s accuracy. An adaptive slicing approach is considering both surface quality and building time, generating hybrid tool paths (Jin et al., 2013) and software package (PowerSHAPE) is performing adaptive direct slicing, where the slicing thickness is according to the curvature of any contour (Sun et al, 2007). Also, Curved Layer Fused Deposition Modelling (CLFDM) and alternatives propose layers of build material to deposit as curved layers following the shape of the part (Singamneni et al. 2014; Lim et al., 2016).

Those approaches may reduce printing time, staircase effect, and improve surface quality, but basically, they are post processes, more focused on improving the manufacturability of an existing geometry than introducing a new design approach especially for 3D printing.

### **Objectives**

The objective of this article is to investigate further the causes and effects of those limitations by physical testing and computer simulations and to integrate them inside the design workflow as driving forces. A set of different solutions are tested, first, in small prototypes and later in real scale to examine the scaling of those effects, since the errors are multiplied. Specifically, by examining design goals simultaneously with manufacturing constraints the method suggests how to avoid or reduce all types of enforcement and support structures, considering printing orientation, and to minimize tool path gaps that appear on the critical double curved locations during the slicing process of the 3D model into 2D contours. In parallel, special effort is taken for the design to be able to reduce traveling time, economizing the amount of interior structural material and total printing time in order to achieve surface continuity and structural stability, by adjusting the seams of the layer paths and infill patterns.

The investigation presents a unified design approach for the design and rapid manufacturing or direct digital manufacturing (Gibson et al., 2010) of end-use large-scale objects, additive manufactured using polyacrylic acid (PLA) pellet material and the Delta WASP 3MT printer provided by Noumena [2]. It is trying to bridge the gap between rapid prototyping and mass production. The process is taking into account all considerations, requirements and post processes for this transition. The objects, especially designed for

3D printing, cannot be mass-produced with other traditional manufacturing technologies (casting, molding, etc.), basically because of the economic cost of a small production. The entire approach is described here as a continuous integrated workflow, from the initial input lines to the generation of tool paths; Input curves, Mesh preparation, Dynamic relaxation, Toolpath optimization.

## Self-Supported Thin Shells

The term thin shell is used here to describe a self-supported structure of thin wall curved surfaces with near zero mean curvature (minimal surfaces). These types of structures have many advantages, like minimizing the amount of material needed and achieving surface continuity which increases structural behavior. The method is based on the simulation of virtual soap films coming from a predefined synthesis of boundary geometries.

Surface tension, a property of liquid surfaces, has physical properties that naturally relax the surface's curvature. It is possible to simulate the surface tension (force per unit length) to a network of curves derived from a given shape. The mean curvature at a point records the net direction of the surface's curvature and gives the force with which surface tension pulls. [3] This is achieved using the Kangaroo2 Physics engine solver [4] which uses dynamic relaxation. 'Goals in Kangaroo can also be based on force-density (in a 1-d element the ratio of force to length). A length goal with target length zero is the same as a constant force-density element, since the tension force is proportional to the length of the line.' [5]. Dynamic relaxation with particle spring systems are used today in structural engineering, especially for pre-stressed nets and membranes and for optimizing the geometry of the connected node positions for network structures (Williams, 2001). Tensile forces could be calculated in warp and weft directions (Figure 1).

Programming the curves of the thin shells as network structure gives the advantage of considering them as structural elements and at the same time, as tooling paths. The method is applied on three predefined topological configurations to achieve both structural behavior and better fabrication results.

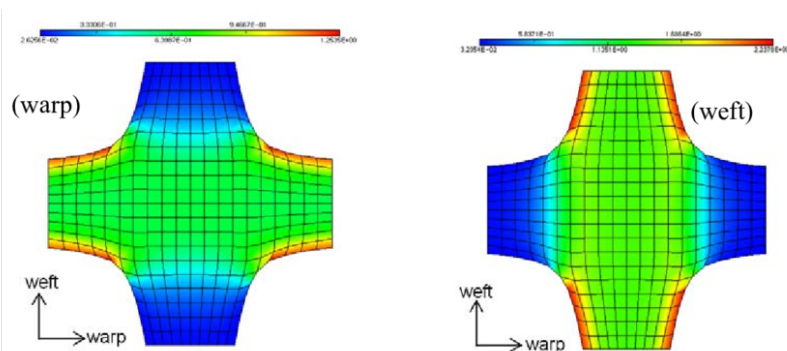


**Figure 1.** Contour of tensile force (a) warp direction and (b) weft direction. (Image taken from: Cherouat A, Borouchaki H. "Present state of the art of composite fabric forming: Geometrical and mechanical approaches". *Materials* (Basel). 2009; 2 (4): 1835–57).

## Methodology

The proposed methodology consists of three design stages: Mesh Construction, Spring-based Dynamic Relaxation and Toolpath Optimization and feedback between them. An initial module was adjusted for fabricating 3 different model typologies of furniture: the first, a *Radiolaria Stool*, based on one module, second, a *Radiolaria Bench*, based on two modules and lastly a *Hyperboloid Chair* made of three modules.

### *Mesh Conversion to Springs*

The conception of the initial module is constructed based on the connection of a sphere with 11 external polygons: 3 lateral hexagons, 6 triangles and 2 top/bottom hexagons (Figure 2, left). The hexagons and triangles polylines are treated in the same manner. First, the connection is made by making a surface between the triangle, projected triangle on the sphere, and a scaled tween curve, half the distance between them (Figure 2, center). In order to find the spring segments, the surface is converted to a mesh made of 4x8 faces (Figure 2, right). The quantity of mesh division of 4, in one direction, is the same for all the polygons, in order to keep the same continuity for all meshes, but the opposite direction varies according to each type of polygon.

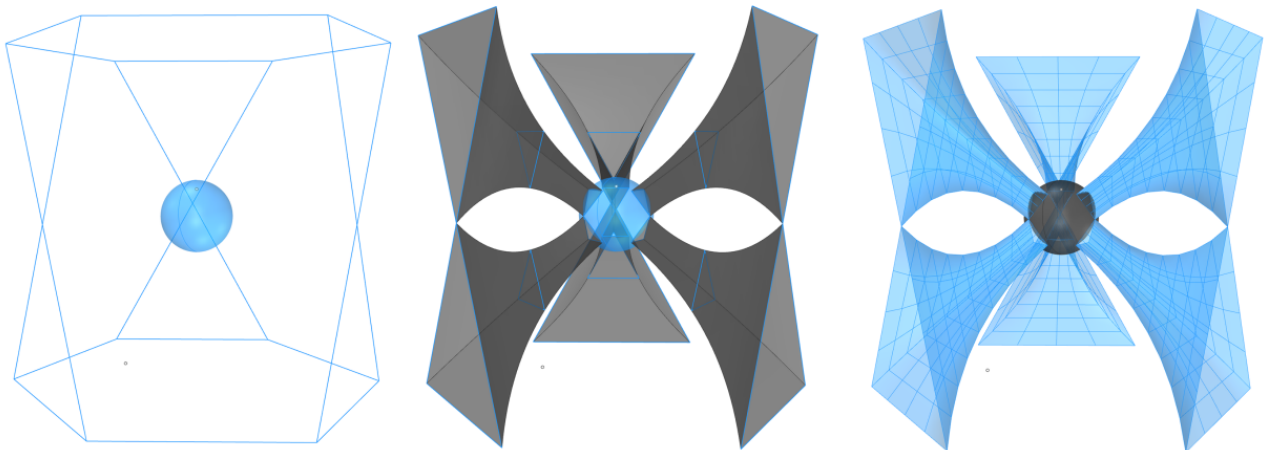


**Figure 2.** (Left) Showing the 3 Lateral Hexagons, 6 Triangles and 2 Top/bottom hexagons with the internal sphere. (Center) image showing the connection of the triangle and the sphere (bridge) generated by the three blue lines. (Right) image showing the mesh generation.

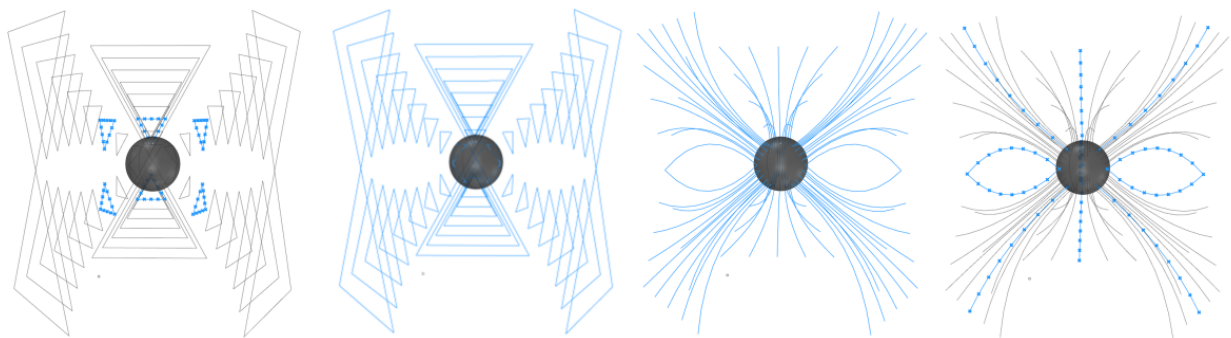


**Figure 3.** Showing the rings (warps) and the ring selected, and the perpendiculars (wefts) and the selected.

The edges from every single face are extracted in 2 sets of lines: the rings (warps) direction and the perpendiculars (wefts) (Figure 3), but one is selected from each in order

later to apply different strength and accomplish a pinching behavior during the relaxation. All these sets of lines are converted to spring systems with the same strength in the Wefts direction and with a length of zero, to keep it minimal. The Warps forces are different for each mesh type. So, the diameter of the mesh of each polygon depends on the quantity of Warps divisions, the Warps strength and the Wefts strength (tensile forces) (Figure 4).

#### *Dynamic Relaxation with Particle Spring System*

Every model typology has different geometrical and dynamical goals, but most of them have 12 anchors per module (Figure 5, left). This single module has an extra goal, that is gravity, in order to move the top and bottom particles in Z direction, for two purposes. One, to allow comfortable sitting on the top and second, to make it easier to 3d print. The final relaxed model (Figure 5, center) is later subdivided twice in order to have more mesh continuity, but with less strength in the anchors to make them stronger. Figure 5, right, shows the pink areas that have less continuity and the red with more mesh continuation.

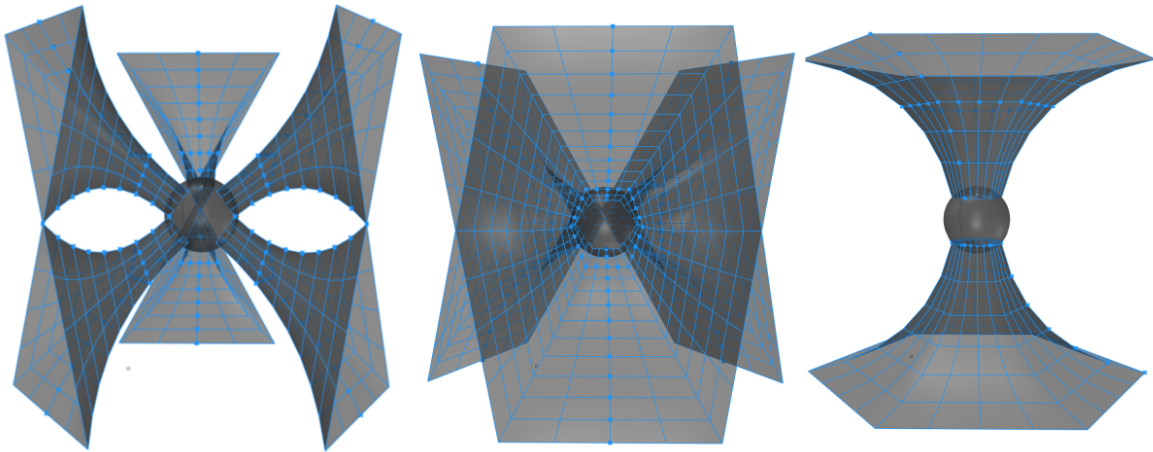


**Figure 4.** Springs from all the polygonal meshes. (Left) Showing projections of triangles to the internal sphere. (Center) Showing the projected lateral hexagons to the sphere. (Right) Showing the projected top and bottom hexagons to the internal sphere.

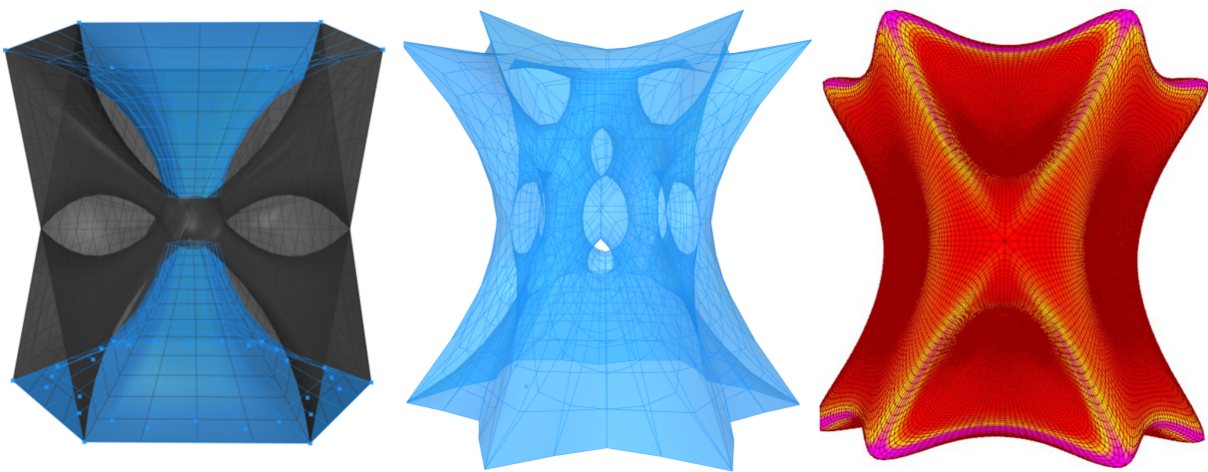


**Figure 5.** (Left) Showing anchor and additional goals. (Center) Final relaxed model (Right) Mean mesh analysis showing continuity between the meshes after the dynamic relaxation, where the red shows more continuous results.



During the dynamic relaxation process, the spring strength in all wefts is the same to allow maximum surface continuity between parts, but in the wraps, strength is different for every generated geometry in order to control various aspects of the manufacturing process. The mean curvature analysis indicates the locations of most discontinuity in pink (Figure 5, right), which are exactly the locations of the anchor points.

The connection parts, after the relaxation process, are similar to ruled surfaces or surfaces of revolution (circular hyperboloids). In fact, they have similar characteristics with the capillary bridges, defined by Plateau (1857), who classified the shapes and investigated their stability. The formation of a liquid concave capillary bridge appears between two particles (Figure 6), or two flat surfaces, or a particle and a surface, because of the attraction or repulsion forces between them which form catenoid shapes (Kralchevsky and Nagayama, 2001).

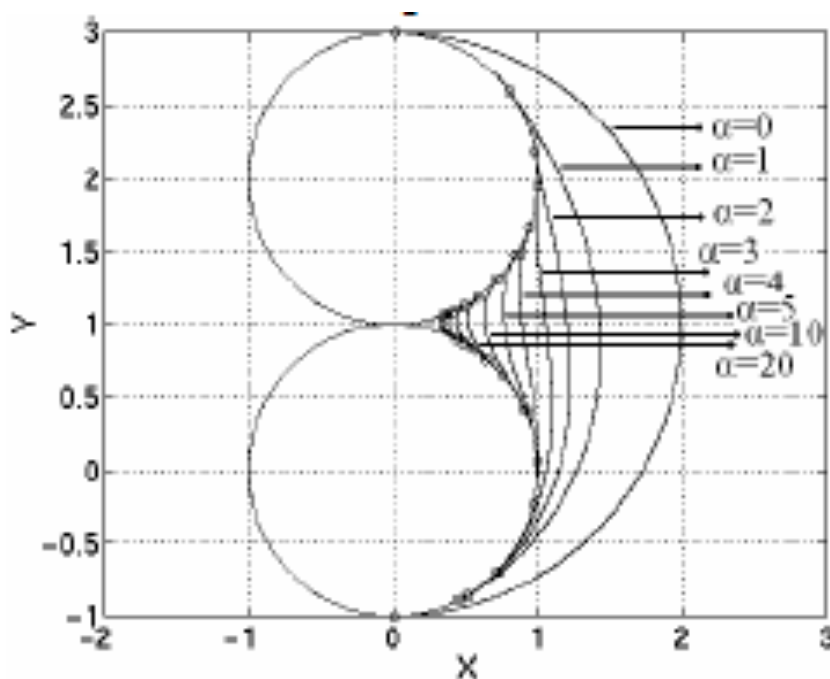


**Figure 6.** Liquid capillary bridge profile between two for values of  $\alpha$  varying constant  $\alpha$ , calculated from equation (Image taken from Heris et al. 2009).

### *Toolpath Optimization*

In general, the method of slicing and sending the G-code to the printer has very generic parameters, but not much for variable layer heights, 3d paths (curved paths), nor custom infill, as the case of most commercial and open-source slicers, like Cura or Simplify3d. Specially, for large 3dprint structures it is crucial to optimize traveling and printing times. As for now, the best solution would have been to keep one single path with no travels, but this limits the designs.

For each experiment, the parametric programming of the toolpaths was different, but in general, the mesh was divided by the inclination of each mesh face according the Z vector (Figure 7, left), and each of the selected mesh areas was treated with different layer height accordingly (see Figure 7, right):

Section A = Top section. 11 layers with 1.2mm height, gradient infill.  
 Section B = Neck section. 10 layers with 1.2 and 1.6mm height, gradient infill.  
 Section C = Support of top surface. 20 layers with 2mm height.  
 Section D = Main body. 292 layers with 1.6 and 1.2mm height.  
 Section E = Feet. 4 layers with 1.6mm height, gradient infill.

The proposed method suggests that by adjusting different values of spring strengths in strategic locations (springs selections) of the mesh projections, it is possible to interactively control the warp and weft (tensile) forces and to adjust the shape of the bridge to fit print criteria (see Figure 8). Consequently, it minimizes the contour line gaps that appear during slicing (see Figure 9). In general, spring forces serve two purposes: Structural performance, as forces in equilibrium achieve surface continuation, and fabrication efficiency, with the adjusted tool paths in the saddle areas.

In order to close the gaps around the saddle areas, there were many different attempts. One was to add some offset paths to fill the selected areas and moderate the staircase effect to reduce the gaps. Another, was to add some paths connecting the paths before the hole. But the one most successful approach was to separate the meshes by the curvature and by adjusting the relaxation springs on the dynamic relaxation, to generate a pinch effect (Figure 8 and 9).

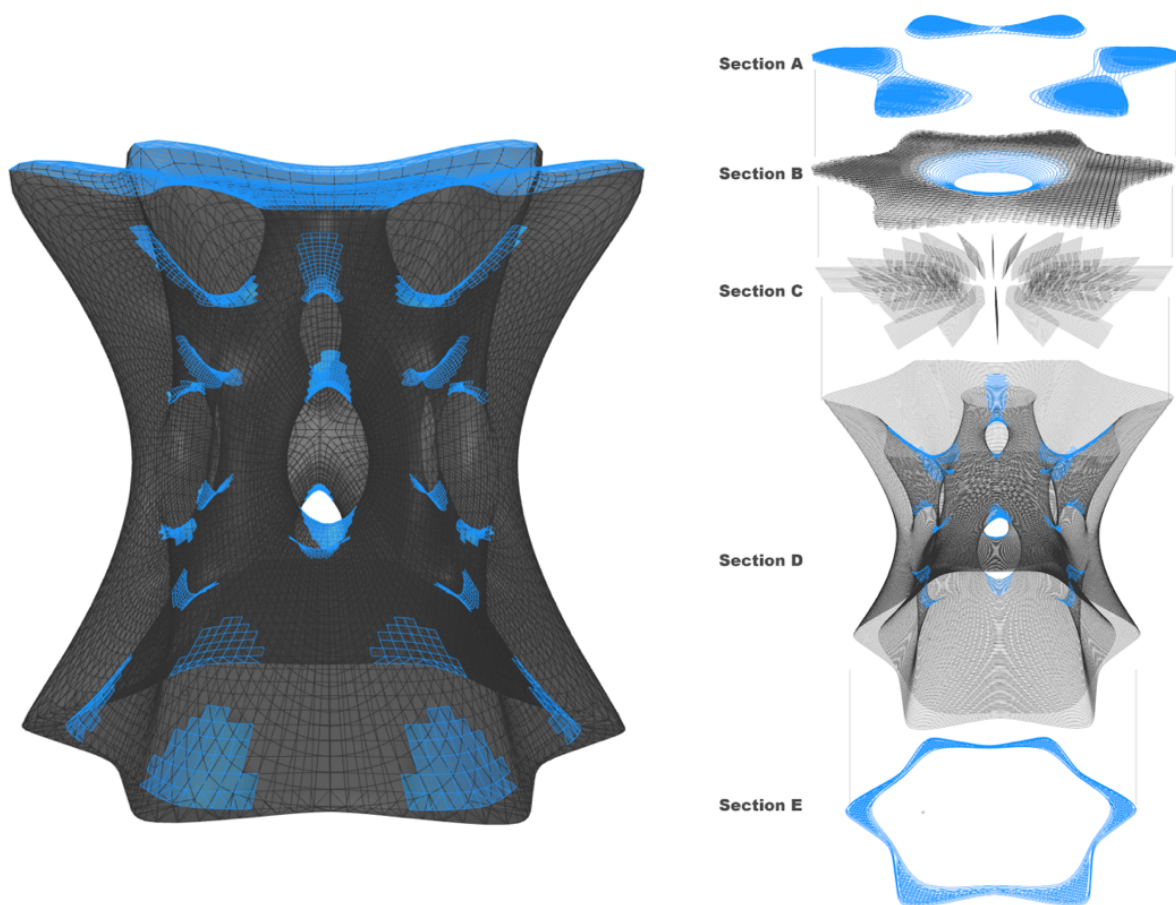


**Figure 7.** Left, showing mesh separation according to the inclination, in blue. Right, final representation of the different types of layer for every part of the structure, in blue the smaller layer heights.



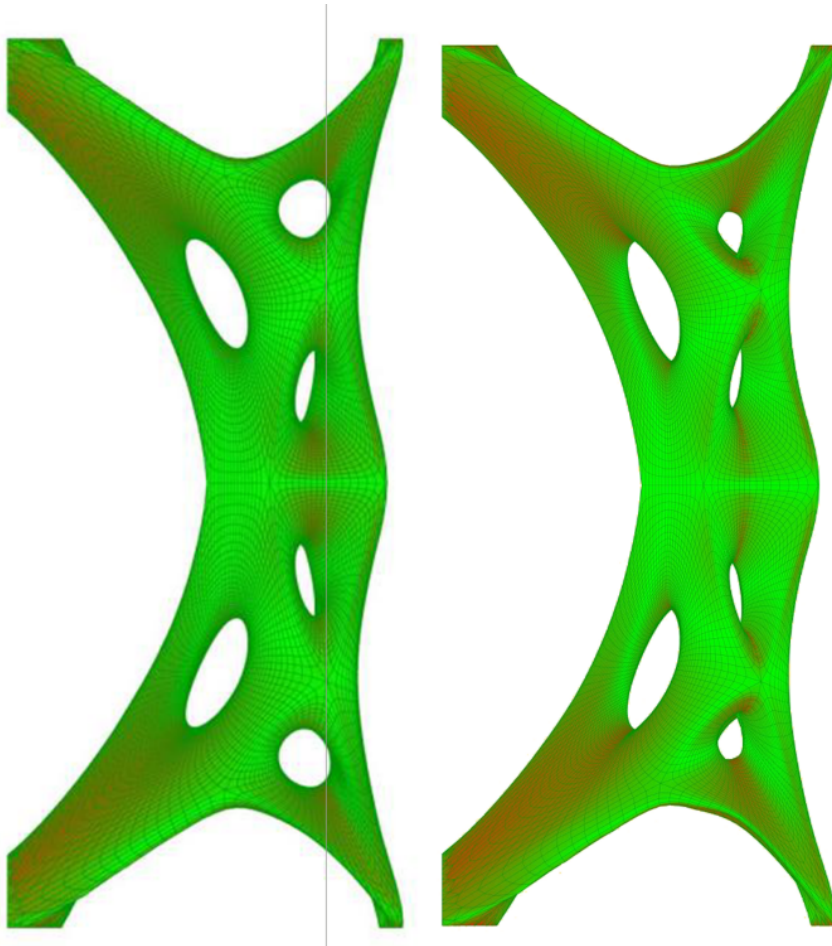


**Figure 8.** Showing in red the mesh angles between each face and the Z vector which are lower than 53 degrees, printed sideways. Mesh geometry Before optimization (left), and After optimization (right).

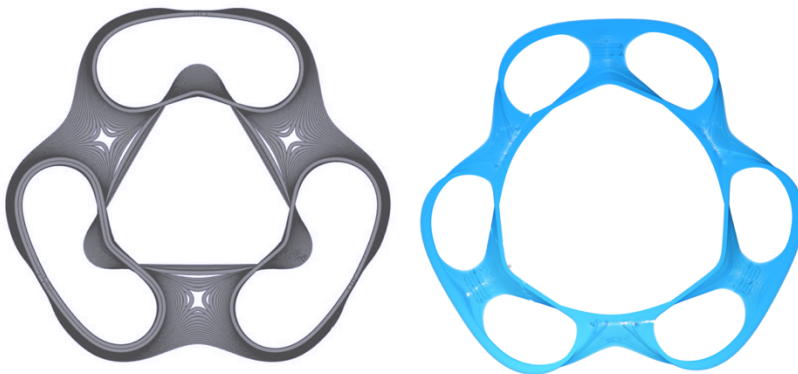


**Figure 9.** Pinch effect. Layer comparison. Left, top view. Section of the object, showing the problem Before around the saddle points, during the simulation with the actual 3mm diameter nozzle and with 1,5 mm layer height (right). Showing the result After applying the mentioned additional forces and the layer modification.

## Case Studies - Radiolaria and Hyperboloid Furniture Series

### *Experiment 1. Radiolaria Stool*

This experiment had a similar relaxation method to the other experiments, but additionally, gravity was applied to the top and bottom vertexes in order to have the bottom printable and the top as a flat sitting area. The stool (Figure 10) is printed vertically, with the main body as a single path. It was divided in many sections in order to have tool path variations of the shells, infills and internal structure.

Characteristics:

- Dimensions: 40 x 44 x 38 cm.
- Main body thickness: 3 mm.
- Material: PLA in Pellet.
- Printing time: 15 hours.
- Toolpath length: 690 m.
- Weight: 15 kilos.



**Figure 10.** © Alberto T. Estévez - GenArqOffice (col. Pablo Baquero, computational designer), *Radiolaria Barcelona Stool*, (printed 1:1 scale by Noumena), *Radiolaria Barcelona Furniture Series/Collection*, iBAG-UIC Barcelona, 2010-2020.

*Experiment 2. Radiolaria Bench*

The second experiment was made of two modules and it had a similar relaxation method to the others experiments; gravity was also applied for the same purposes. The springs strengths of ring division were also adapted depending on the meshes. The bench (Figure 11) has been printed sideways in order to use all the height available of the printer; The main body as a single shell path, and divided in many sections in order to have variation on the shell's toolpaths, infills and internal structure.



**Figure 11.** © Alberto T. Estévez - GenArqOffice (col. Pablo Baquero, computational designer), *Radiolaria Barcelona double Bench*, (printed 1:1 scale by Noumena), *Radiolaria Barcelona Furniture Series/Collection*, iBAG-UIC Barcelona, 2019.

#### Characteristics:

- Dimensions: 40 x 90 x 45 cm.
- Main body thickness: 1 shell (3 mm).
- Material: PLA in Pellet.
- Printing time: 37 hours.
- Toolpath length: 2,8 km.
- Weight: 21 kilos.

#### *Experiment 3. Hyperboloid Chair*

The last experiment was made of three modules, sectioned from both sides and it had the same relaxation method to the others experiments; Some Pull to Curve goals were used, but not gravity. The springs strengths quantity of ring division was also changed depending on the meshes of each module. The chair (Figure 12) has been printed sideways in order to fit the three modules on the printer, with the main body as dual shell path.

#### Characteristics:

- Dimensions: 60 x 70 x 55 cm.
- Main body thickness: 1 shell (3mm).
- Material: PLA in Pellet.
- Printing time: 37 hours.
- Toolpath length: 3 km.
- Weight: 21 kilos.



**Figure 12.** © Alberto T. Estévez - GenArqOffice (col. Pablo Baquero, computational designer), *Hyperboloid Barcelona Chair* (printed 1:1 scale by Noumena), *Hyperboloid Barcelona Furniture Series/Collection*, iBAG-UIC Barcelona, 2019.

#### Conclusion

This article presents an integrated design methodology using dynamic relaxation to fulfil design goals and manufacturing constraints simultaneously. By examining current AM limitations and considerations for large scale FFF, it demonstrates a continuous generative workflow, from initial lines to the printing toolpaths, focusing on locating the areas with the most difficulty for manufacturing, such as the saddle surfaces and adjusting the design. The outcomes present a series/collection of furniture. The design



began the year 2010 until today, done by Alberto T. Estévez with his collaborators of the GenArqOffice (Genetic Architectures Research Group & Office), integrate on the iBAG-UIC Barcelona (Institute for Biodigital Architecture & Genetics). In the case of these three designs presented here, they were also made with the collaboration of Pablo Baquero as computational designer and of Noumena for the digital fabrication (Figure 13).

This research manifests that with the use of emergent technologies, the designer/architect does not only need to depend on the manufacturer's skills, having actual control of the post processes, but it's possible with the computational tools to expand design for manufacturing systems. For this, it would need expertise, knowledge and education to support it (Estévez, 2015).



**Figure 13.** © Alberto T. Estévez - GenArqOffice (col. Pablo Baquero, computational designer), *Hyperboloid Barcelona Chair* (printed 1:1 scale by Noumena), *Radiolaria* and *Hyperboloid Barcelona Furniture Series/Collection*, iBAG-UIC Barcelona, 2010-2020.

## References

- Alsoufi, M. S. & Elsayed, A. E. (2017) "Warping deformation of desktop 3D printed parts manufactured by open-source fused deposition modelling (FDM) system". *International Journal of Mechanical and Mechatronics Engineering*, vol. 17, n. 4, pp. 7-16.
- Chacón, J. M., et al. (2017) "Additive Manufacturing of PLA structures using Fused Deposition Modelling: Effect of process parameters on mechanical properties and their optimal selection". *Materials and Design*, vol. 124, pp. 143-157.
- Estévez, A. T. (2015) *Biodigital Architecture & Genetics: Writings / Escritos*, ESARQ-UIC Barcelona, Barcelona.
- Gibson, I., Rosen, D., & Stucker, B. (2010) "Direct Digital Manufacturing". *Additive Manufacturing Technologies*. Springer, Boston, MA.
- Gupta, S. K. et al. (1997) "Automated manufacturability analysis: A survey". *Research in Engineering Design*, vol. 9, n. 3, pp. 168-190, Springer.
- Gupta, P. & Krishnamoorthy, B. (2019) "Continuous toolpath planning in Additive Manufacturing", pp. 1-31. Available at: <http://arxiv.org/abs/1908.07452>.
- Heris, S., Zeinali, H., Mosavian, M. T., & White, E. T. (2009) "Capillary holdup between vertical spheres". *Brazilian Journal of Chemical Engineering*, vol. 26, n. 4, pp. 695-704.
- Huang, A. (2016) "From bones to bricks. Synthesis, design and architecture. Designing the 3D printed Durotaxis Chair and La Burbuja Lamp". In VV.AA., *Posthuman Frontiers: Data, Designers, and Cognitive Machines; Proceedings of the 36th ACADIA*, pp. 318-325.
- Jin, Y. A., He, Y., & Fu, J. Z., (2013) "An adaptive tool path generation for fused deposition modeling". *Advanced Materials Research*, vol. 819, pp. 7-12.

Kralchevsky, P. & Nagayama, K. (2001) "Capillary bridges and capillary-bridge forces". *Studies in Interface Science*, vol.10C, pp. 469-502.

Lim, S., et al. (2016), "Modelling curved-layered printing paths for fabricating large-scale construction components". *Journal of Additive Manufacturing, Special Issues: Modeling and Simulation*, vol. 12B, pp. 216-230.

Marchment, T., Sanjayan, J. & Xia, M. (2019) "Method of enhancing interlayer bond strength in construction scale 3D printing with mortar by effective bond area amplification", *Materials and Design*, vol. 169.

Nasr, E. S. A., Al-Ahmari, A. & Moiduddin, K. (2014) "CAD Issues in Additive Manufacturing". In Hashmi, S. et al. (ed.). *Comprehensive Materials Processing*, vol. 10, pp. 375-399, Elsevier.

Plateau, J. (1857) I. "Experimental and theoretical researches on the figures of equilibrium of a liquid mass withdrawn from the action of gravity". *The London, Edinburgh, and Dublin Philosophical Magazine and Journal of Science*, S. 4, vol. 14, n. 90, pp. 1-22.

Roschli, A. et al. (2019) "Creating toolpaths without starts and stops for extrusion-based systems". In VV.AA., *30th Annual International Solid Freeform Fabrication Symposium*, pp. 1113-1125.

Simpson, T.W (2019) "Designing for Additive Manufacturing". In Bandyopadhyay A. & Bose S. (eds.) *Additive Manufacturing*, pp. 261, CRC Press.

Sun, S. H., Chiang, H. W. & Lee, M. I. (2007) "Adaptive direct slicing of a commercial CAD model for use in rapid prototyping", *International Journal of Advanced Manufacturing Technology*, vol. 34, n. 7-8, pp. 689-701.

Singamneni, S. et al. (2010) "Curved layer fused deposition modelling", *Journal for New Generation Sciences*, vol. 8, n. 2, pp. 95-107.

Thompson, M. K. et al. (2016) "Design for Additive Manufacturing: Trends, opportunities, considerations, and constraints", *CIRP Annals*, vol. 65, n. 2, pp. 737-760, Elsevier BV.

Williams, C. J. K. (2001) "The analytic and numerical definition of the geometry of the British Museum Great Court Roof". In Burry, M., et al. (eds.). *Mathematics & design*, pp. 434-440, Deakin University, Australia.

[1] The effect of layer bonding on the strength of 3D printed structures.  
<https://ukdiss.com/examples/effect-layer-bonding-3d-printed-structures.php?vref=1>.

[2] Wasp Hub Barcelona. <https://noumena.io/wasphub/>.

[3] Minimal surfaces. <https://wewantttolearn.wordpress.com/category/resources/software/grasshopper>.

[4] Kangaroo 2. Version 2.3.3. Released on 2019-Dec-15. Created by Daniel Piker.  
<https://grasshopperdocs.com/addons/kangaroo-2.html>.

[5] Reply by Daniel Piker on February 20, 2017.  
<https://www.grasshopper3d.com/group/kangaroo/forum/topics/force-density-method-on-kangaroo>.